

## Influence of preparation method on structural and magnetic properties of nickel ferrite nanoparticles

BINU P JACOB, ASHOK KUMAR<sup>†</sup>, R P PANT<sup>†</sup>, SUKHVIR SINGH<sup>†</sup> and E M MOHAMMED\*

Department of Physics, Maharaja's College, Ernakulam 681 011, India

<sup>†</sup>National Physical Laboratory, New Delhi 110 012, India

MS received 15 May 2010

**Abstract.** Nickel ferrite nanoparticles of very small size were prepared by sol–gel combustion and co-precipitation techniques. At the same annealing temperature sol–gel derived particles had bigger crystallite size. In both methods, crystallite size of the particles increased with annealing temperature. Sol–gel derived nickel ferrite particles were found to be of almost spherical shape and moderate particle size with a narrow size distribution; while co-precipitation derived particles had irregular shape and very small particle size with a wide size distribution. Nickel ferrite particles produced by sol–gel method exhibited more purity. Sol–gel synthesized nanoparticles were found to be of high saturation magnetization and hysteresis. Co-precipitation derived nickel ferrite particles, annealed at 400°C exhibited superparamagnetic nature with small saturation magnetization. Saturation magnetization increased with annealing temperature in both the methods. At the annealing temperature of 600°C, co-precipitation derived particles also became ferrimagnetic.

**Keywords.** Nickel ferrite; sol–gel technique; co-precipitation; superparamagnetism.

### 1. Introduction

During the last few years, ferrite nanoparticles have drawn major attention because of their technological importance in high density magnetic storage, electronic and microwave devices, telecommunication equipments, magnetic fluids, magnetically guided drug delivery and gas sensors (Murdock *et al* 1992; Kim *et al* 2001; Sanyanarayana *et al* 2003; Mishra *et al* 2006; Rana *et al* 2007; Kharabe *et al* 2008). Among various ferrites, which form a major constituent of the magnetic ceramic materials, nanosized nickel ferrite possesses attractive properties for the application as soft magnets, core materials in power transformers and low loss materials at high frequencies (Abraham 1994). High permeability in the radio frequency region, high electrical resistivity, high Curie temperature and low eddy current loss are important properties of nickel ferrites, which make them suitable for wide range of applications (Singhal and Chandra 2007). Being a technologically important material, Ni-ferrites as well as Ni-based mixed ferrites are extensively investigated by various researchers (Mishra *et al* 2006; Ebrahimi and Azadmanjiri 2007; Zahi *et al* 2007; Maaz *et al* 2009).

Nickel ferrite has inverse spinel structure. The crystal structure is face centred cubic with the unit cell contain-

ing 32 O<sup>2-</sup>, 8 Ni<sup>2+</sup> and 16 Fe<sup>3+</sup> ions. The oxygen ions form 64 tetrahedral and 32 octahedral sites, where 24 cations are distributed. The eight Ni<sup>2+</sup> and eight Fe<sup>3+</sup> cations occupy half of the octahedral sites and the other eight Fe<sup>3+</sup> ions occupy eight tetrahedral sites (Smit and Wijn 1959; Giannakopoulou *et al* 2002). Ferrimagnetic property of the material arises from magnetic moments of anti-parallel spins between Fe<sup>3+</sup> ions at tetrahedral sites and Ni<sup>2+</sup> and Fe<sup>3+</sup> ions at octahedral sites (Patil and Chougule 2009). The properties of ferrite nanoparticles are influenced by the composition and microstructure which are sensitive to the preparation methodology used. Ferrite nanoparticles are usually prepared by various physical and chemical methods like mechanical milling, inert gas condensation, hydrothermal reaction, ceramic method, sol–gel and co-precipitation techniques etc (Mishra *et al* 2006; Ebrahimi and Azadmanjiri 2007; Zahi *et al* 2007; Maaz *et al* 2009). Sol–gel method has the advantage of good stoichiometric control and the production of ultrafine particles with a narrow size distribution, in a relatively short processing time. Advantages of co-precipitation are the high production rate, very small particle size, low temperature, etc. In order to see the role of different synthesis techniques on the growth, structural morphology and magnetic properties of Ni-ferrite, in the present work, we synthesized ultrafine nickel ferrite nanoparticles by sol–gel and co-precipitation methods and their structural and magnetic properties were thoroughly investigated.

\*Author for correspondence (emmoammed\_2005@yahoo.com)

## 2. Experimental

### 2.1 Synthesis

In sol-gel synthesis, stoichiometric ratios of AR grade ferric nitrate ( $\text{Fe}(\text{NO}_3)_3 \cdot 9\text{H}_2\text{O}$ ) and nickel nitrate ( $\text{Ni}(\text{NO}_3)_2 \cdot 6\text{H}_2\text{O}$ ) (99.9% pure MERK) were dissolved in minimum amount of ethylene glycol at room temperature and the sol was heated at  $60^\circ\text{C}$  to form a wet gel. The gel then dried at  $120^\circ\text{C}$  self ignites to form  $\text{NiFe}_2\text{O}_4$  powder. The combustion can be considered as a thermally induced redox reaction of the gel wherein ethylene glycol acts as a reducing agent. The nitrate ion acts as an oxidant. The nitrate ion provides an *in situ* oxidizing environment for the decomposition of the organic component. The obtained powder ground well and two different portions were annealed for 2 h at 400 and  $600^\circ\text{C}$ , respectively using a carbolite furnace.

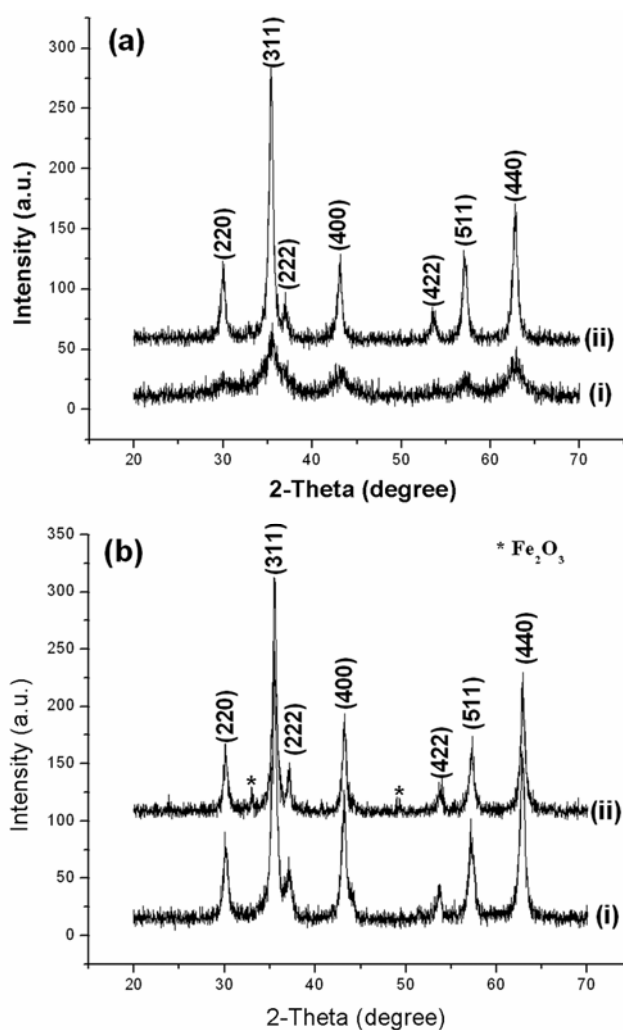
In co-precipitation technique, appropriate amount of ferric nitrate and nickel nitrate were dissolved in sufficient amount of de-ionized water. In order to control the pH, three molar sodium hydroxide, which acts as the precipitating agent was added to the solution kept under constant stirring. Brown coloured precipitate formed was filtered and washed several times using de-ionized water until its pH becomes neutral and dried at  $200^\circ\text{C}$  for 1 h. The product was then milled in an agate mortar and two different portions were annealed at 400 and  $600^\circ\text{C}$ , respectively for 2 h to form fine Ni-ferrite nanoparticles.

### 2.2 Characterization

The crystalline phases of the prepared samples were identified by X-ray diffraction (XRD) technique using RIGAKU make RINT 2000 powder X-ray diffractometer with  $\text{CuK}\alpha$  radiation ( $\lambda = 1.54059 \text{ \AA}$ ) at 40 kV and 30 mA. Scanning was performed from  $20^\circ$  to  $70^\circ$  at a step size of  $0.02^\circ/\text{s}$  for each sample. The crystal structure, lattice parameter, crystallite size and X-ray density were determined. Elemental analysis of the samples prepared by both methods was carried out using energy dispersive X-ray spectroscopy (EDX) (OXFORD-INCA-ENERGY 250). The Fourier transform infrared (FTIR) absorption spectra of the samples were recorded using FTIR spectrometer (Thermo Nicolet, Avatar 370) in the wave number range  $4000\text{--}400 \text{ cm}^{-1}$  with potassium bromide (KBr) as solvent. High resolution transmission electron microscope (HRTEM, TECHNAI  $G^2$  F30 STWIN) operated at 300 kV was used to investigate the morphology and particle size of the synthesized Ni-ferrite samples. Magnetic characterization was carried out using vibrating sample magnetometer (VSM, PAR EG&G 4500) at room temperature up to a maximum field of 15 kOe.

## 3. Results and discussion

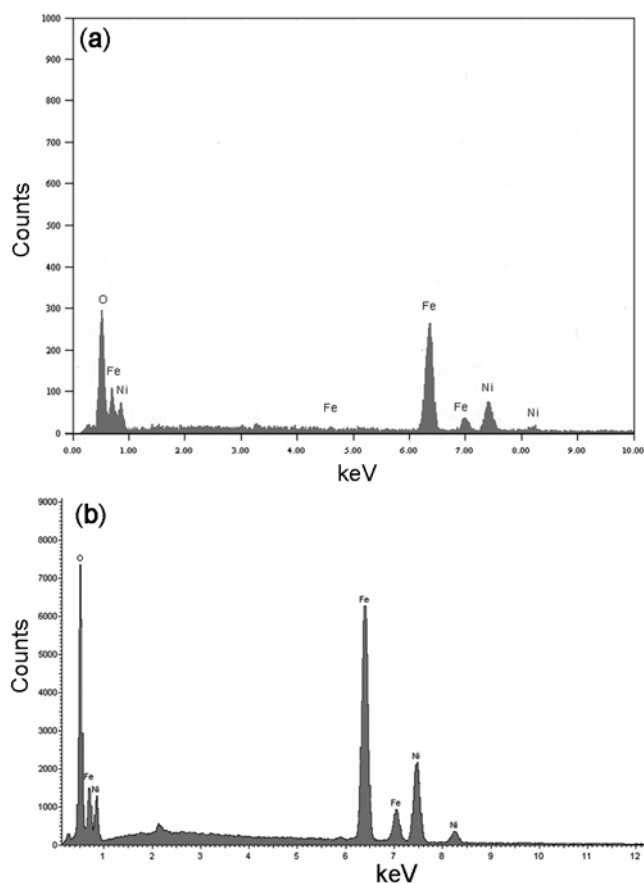
Figure 1 shows XRD patterns of  $\text{NiFe}_2\text{O}_4$  (a) co-precipitation derived samples and (b) sol-gel derived samples. The patterns were compared with standard data (JCPDS PDF card No. 074-2081) and the formation of single phase cubic  $\text{NiFe}_2\text{O}_4$  nanoparticles in all the samples was confirmed. Sol-gel derived sample annealed at  $600^\circ\text{C}$  shows some extra peaks (figure 1b) indicating the formation of hematite ( $\text{Fe}_2\text{O}_3$ ) at this temperature. The mean crystallite sizes of particles were calculated for all samples using Scherrer formula (Cullity 1978). The average crystallite sizes of the samples are tabulated in table 1. It is obvious from the table that co-precipitation yields Ni-ferrite nanoparticles with less crystallite size compared with sol-gel synthesis. Similar results were reported earlier in the case of magnesium ferrite (Liu *et al* 2007). At the annealing temperature of  $600^\circ\text{C}$ , both the



**Figure 1.** X-ray diffraction patterns of  $\text{NiFe}_2\text{O}_4$  nanoparticles prepared by (a) co-precipitation, annealed at (i)  $400^\circ\text{C}$  and (ii)  $600^\circ\text{C}$  and (b) sol-gel, annealed at (i)  $400^\circ\text{C}$  and (ii)  $600^\circ\text{C}$ .

**Table 1.** XRD analysis and magnetic characterization results of NiFe<sub>2</sub>O<sub>4</sub> samples.

Preparation technique	Annealed temperature (°C)	Crystallite size (nm)	X-Ray density (g/cc)	Lattice constant (Å)	Saturation magnetization $M_S$ (emu/g)	Remanence $M_R$ (emu/g)	Coercivity $H_C$ (Oe)
Sol-gel	400	15-100	5.2831	8.3807	30.8377	3.2500	86.6648
	600	16.700	5.2790	8.3711	31.6259	3.8800	113.9953
Co-precipitation	400	5.165	5.2862	8.3720	14.2219	–	–
	600	15.009	5.2201	8.3804	30.8990	1.5854	38.7849

**Figure 2.** EDX spectra of NiFe<sub>2</sub>O<sub>4</sub> nanoparticles prepared by (a) co-precipitation and (b) sol-gel technique.

methods give almost the same crystallite size. Thus sol-gel derived particles attain better crystallinity even at lower annealing temperature. In sol-gel as well as co-precipitation, the crystallite size was observed to be increasing with temperature. It was reported earlier that annealing process generally decreases lattice defects and strains; however, it can also cause coalescence of smaller grains that results in an increase in the average grain size of nanoparticles (Raming *et al* 2002). The actual (X-ray) density of NiFe<sub>2</sub>O<sub>4</sub> nanoparticles is calculated using the formula (Khan *et al* 2009)

$$P_x = 8M/Na^3, \quad (1)$$

and is given in table 1. Where  $M$  is the molecular weight (kg) of the sample,  $N$  the Avogadro's number (per mol) and  $a$  the lattice constant (Å). X-ray density is observed to be less than that reported for nickel ferrite produced by ceramic technique; but it is greater than physical density of Ni-ferrite which is in accordance with literature (Khan *et al* 2009). Calculated values of lattice parameter of Ni-ferrite samples are listed in table 1, which are in close agreement with standard data (8.34 Å) (Smit and Wijn 1959).

The stoichiometry of the powder samples in both the methods was checked by EDX analysis. EDX patterns of the samples are shown in figure 2 and composition of the elements present is given in table 2. Sol-gel derived sample shows expected stoichiometry; while co-precipitation derived sample indicates nickel deficiency and the presence of excess oxygen. Co-precipitation yields NiFe<sub>2</sub>O<sub>4</sub> particles of very small size and hence specific surface area of the particles becomes very large. So the possibility of oxygen adsorption is high and this may be the reason for excess oxygen (Yang *et al* 2005). No trace of any impurity was found which indicates purity of the samples.

Morphology and particle size of the synthesized samples were investigated using HRTEM. Figure 3 shows HRTEM images of Ni-ferrite nanoparticles synthesized by (a) co-precipitation and (b) sol-gel techniques, annealed at 400°C. From figure 3(a) it is observed that sol-gel derived particles are slightly agglomerated with almost spherical shape and a particle size of 18–25 nm, which confirm the XRD analysis. Co-precipitation derived particles are of irregular shape with a wide particle size distribution of 8–20 nm. Thus, it is evident that sol-gel synthesis gives Ni-ferrite particles of moderate size and a narrow particle size distribution.

FTIR spectral analysis helps to confirm the formation of spinel structure in ferrite samples. The FTIR spectra of the investigated NiFe<sub>2</sub>O<sub>4</sub> samples are shown in figure 4. In the wavenumber range of 1000–300 cm<sup>-1</sup>, two main broad metal-oxygen bands are seen in the infrared spectra of all spinels, especially ferrites. The higher one ( $\nu_1$ ) generally observed in the range 600–550 cm<sup>-1</sup>, is caused by the stretching vibrations of the tetrahedral metal-oxygen bond. The lowest band ( $\nu_2$ ) usually observed in the range 450–385 cm<sup>-1</sup>, is caused by the metal-oxygen

vibrations in the octahedral sites (Waldron 1955). The vibrational frequencies of IR bands  $\nu_1$  and  $\nu_2$  of samples prepared by both co-precipitation and sol-gel are given in table 3, which are in perfect agreement with reported values (Montemayor *et al* 2007; Priyadharsini *et al* 2009).

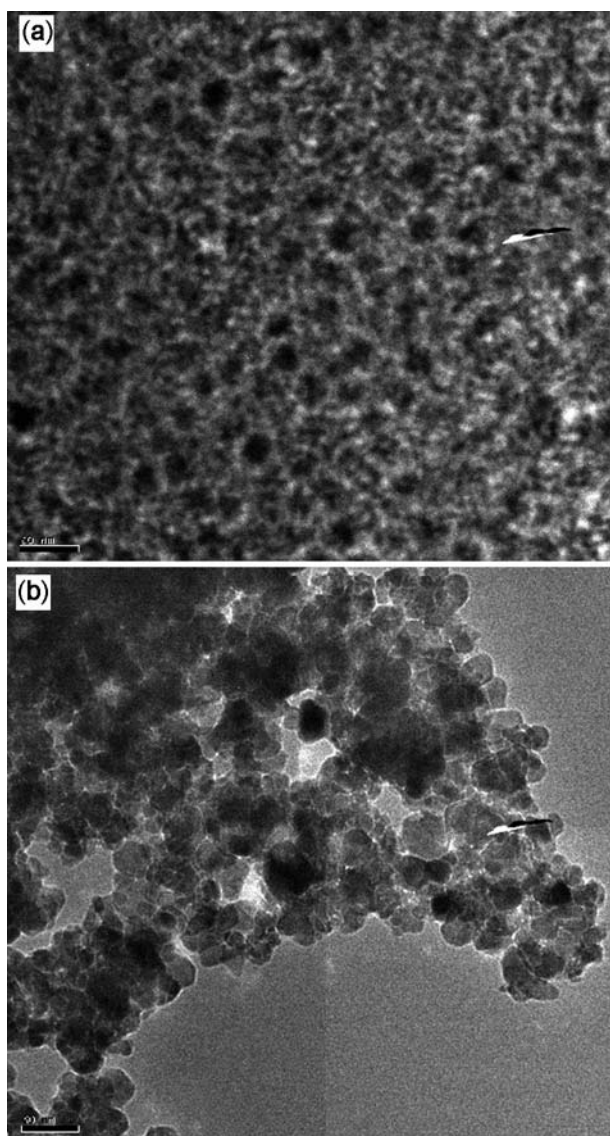


**Figure 3.** TEM micrograph of  $\text{NiFe}_2\text{O}_4$  nanoparticles prepared by (a) co-precipitation, annealed at  $400^\circ\text{C}$  and (b) sol-gel technique, annealed at  $400^\circ\text{C}$ .

**Table 2.** EDX results of  $\text{NiFe}_2\text{O}_4$  samples prepared by co-precipitation and sol-gel techniques.

Element present	Co-precipitation		Sol-gel	
	Expected	EDX	Expected	EDX
Ni	1	0.4529	1	0.9933
Fe	2	1.3678	2	1.8865
O	4	5.1793	4	4.1209

The spectra show prominent bands near  $3400$  and  $1600\text{ cm}^{-1}$ , which are attributed to the stretching modes and H-O-H bending vibrations of the free or absorbed water. The band near  $1400\text{ cm}^{-1}$  is due to the anti-symmetric NO-stretching vibrations arising from the nitrate group which is present as residue in the samples (Priyadharsini *et al* 2009). This band is very weak in the spectra of sol-gel derived sample, indicating the purity of Ni-ferrite nanoparticles synthesized by this method.

Magnetic characterization of the samples was performed by VSM at room temperature with a maximum applied field of 15 kOe. Figure 5 shows typical magnetic hysteresis loops of Ni-ferrite samples prepared by (a) co-precipitation, annealed at  $400^\circ\text{C}$ , (b) co-precipitation, annealed at  $600^\circ\text{C}$ , (c) sol-gel, annealed at  $400^\circ\text{C}$  and (d) sol-gel, annealed at  $600^\circ\text{C}$ . It is obvious from the figure that saturation magnetization ( $M_S$ ) is not attained even in the maximum field of 15 kOe. The  $M_S$  values of all the samples were calculated by extrapolating the inverse of the field vs magnetization ( $M$ ) graph to  $1/H = 0$  (Kale *et al* 2004). The saturation magnetization ( $M_S$ ), coercivity ( $H_C$ ) and remanence ( $M_R$ ) of all the samples are given in table 1. It is observed that co-precipitation derived Ni-ferrite particles annealed at  $400^\circ\text{C}$  do not exhibit hysteresis with almost immeasurable remanence and coercivity. This is a unique property of superparamagnetism (Leslie-Pelecky and Riek 1996). When annealed at  $600^\circ\text{C}$ ,

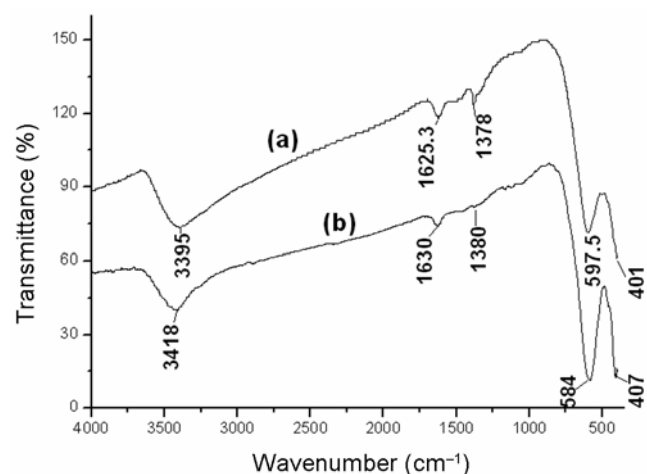


**Figure 4.** FTIR spectra of Ni-ferrite nanoparticles, annealed at  $400^\circ\text{C}$  prepared by (a) co-precipitation method and (b) sol-gel technique.

**Table 3.** FTIR frequency bands of  $\text{NiFe}_2\text{O}_4$  samples.

Preparation technique	IR frequency bands ( $\text{cm}^{-1}$ )	
	$\nu_1$	$\nu_2$
Co-precipitation	401	597.5
Sol-gel	407	584

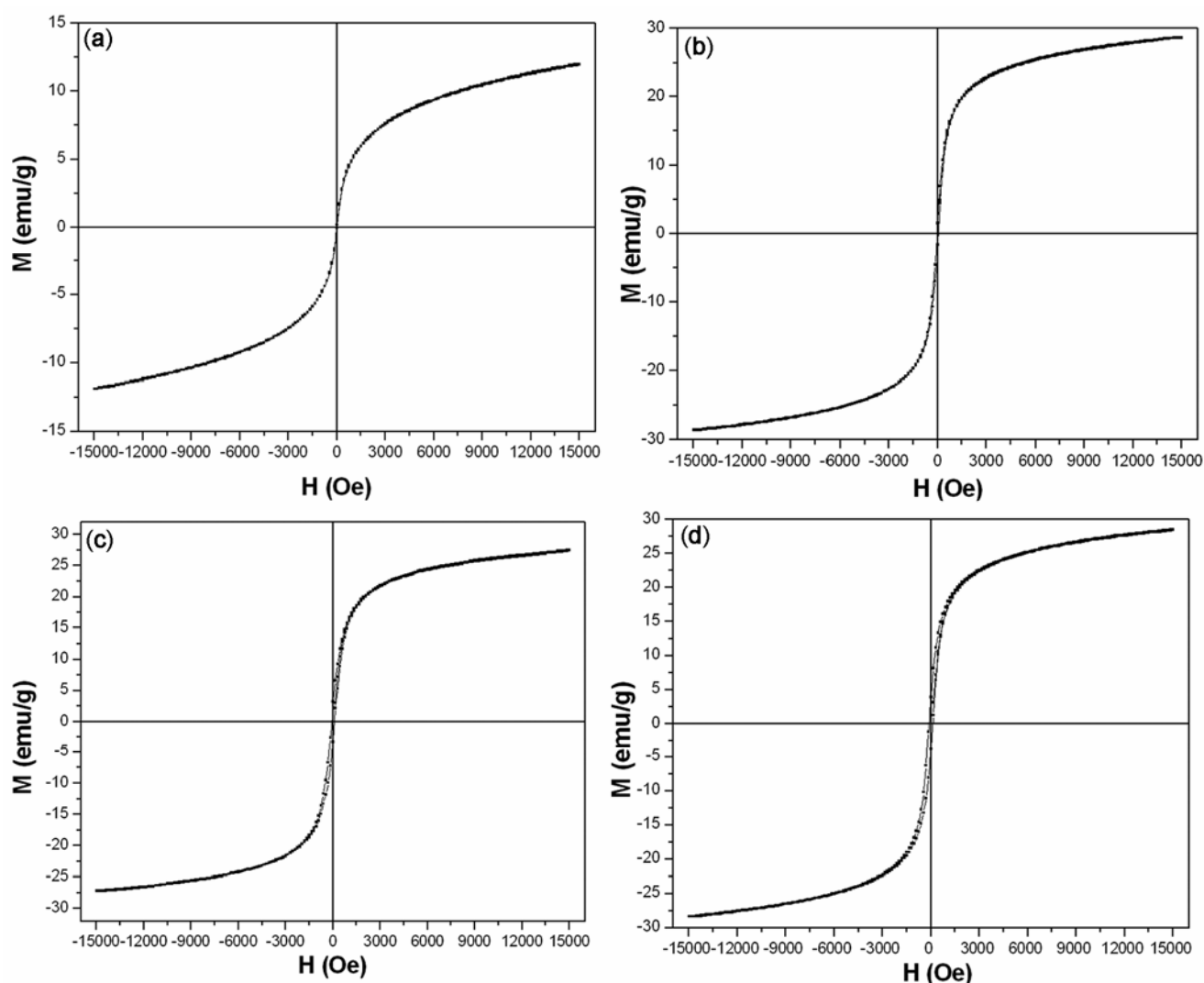


**Figure 5.** Room temperature hysteresis loop of  $\text{NiFe}_2\text{O}_4$  nanoparticles prepared by (a) co-precipitation, annealed at  $400^\circ\text{C}$ , (b) co-precipitation, annealed at  $600^\circ\text{C}$ , (c) sol-gel technique, annealed at  $400^\circ\text{C}$  and (d) sol-gel technique, annealed at  $600^\circ\text{C}$ .

co-precipitation derived particles also exhibit hysteresis. This is expected since at higher temperature, there is increase in particle size as it is clear from XRD analysis. Co-precipitation derived sample annealed at  $600^\circ\text{C}$  has very small  $M_R$  and  $H_C$  values but almost equal  $M_S$  value compared with the corresponding sol-gel derived sample. Sol-gel derived samples are ferrimagnetic with moderately high saturation magnetization. Comparatively low of  $M_S$  value of sol-gel derived sample annealed at  $600^\circ\text{C}$  may be due to the presence of  $\text{Fe}_2\text{O}_3$ . The low value of saturation magnetization compared with that of bulk Ni-ferrite ( $56 \text{ emu/g}$ ) (Maaz *et al* 2009) can be understood on the basis of core-shell model, which explains that the finite size effects of the nanoparticles lead to a canting of spins on their surface and thereby reduces its magnetization (Kodama 1999; Priyadharsini *et al* 2009).

#### 4. Conclusions

Co-precipitation and sol-gel techniques have been used to synthesize  $\text{NiFe}_2\text{O}_4$  nanoparticles. Both the methods produce single phase cubic Ni-ferrite nanoparticles; but sol-gel derived particles annealed at  $600^\circ\text{C}$  exhibits hematite ( $\text{Fe}_2\text{O}_3$ ) phase also. Co-precipitation gives particles of very small size with a wide size variation (8–20 nm) and superparamagnetic nature. Sol-gel combustion produces Ni-ferrite particles of comparatively larger size with small size variation (18–25 nm) and ferrimagnetic nature. As the annealing temperature is increased, particle size and saturation magnetization are found to increase in both the methods. Co-precipitation derived sample also exhibits hysteresis at the annealing temperature of  $600^\circ\text{C}$ . Sol-gel method is better for the preparation of homogeneous, pure and compositionally

stoichiometric ferrites. Co-precipitation is suitable for the synthesis of ferrites with very small size and superparamagnetic nature. At the same annealing temperature, co-precipitation derived  $\text{NiFe}_2\text{O}_4$  nanoparticles exhibit less hysteresis loss with almost same saturation magnetization.

### Acknowledgement

One of the authors (BPJ) is grateful to the University Grants Commission, New Delhi, for providing a FIP fellowship. (EMM) thanks UGC for financial support for this research work.

### References

- Abraham T 1994 *Am. Ceram. Soc. Bull.* **73** 62
- Cullity B D 1978 *Elements of X-ray diffraction* (California: Addison-Wesley) 2nd edn, p. 102
- Ebrahimi S A S and Azadmanjiri J 2007 *J. Non-Cryst. Solids* **353** 802
- Giannakopoulou T, Kompotiatis L, Kontogeorgakos A and Kordas G 2002 *J. Magn. Magn. Mater.* **246** 360
- Kale A, Gubbala S and Misra R D K 2004 *J. Magn. Magn. Mater.* **277** 350
- Khan M A, Islam M U, Rahman I Z, Genson A and Hampshire S 2009 *Mater. Charact.* **60** 73
- Kharabe R G, Devan R S, Kanamadi C M and Chougule B K 2008 *J. Alloys Compds* **463** 67
- Kim Woo Chul, Kim Sam Jin, Lee Seung Wha and Kim Chul Sung 2001 *J. Magn. Magn. Mater.* **226** 1418
- Kodama R H 1999 *J. Magn. Magn. Mater.* **200** 359
- Leslie-Pelecky Diandra L and Riek Reuben D 1996 *Chem. Mater.* **8** 1770
- Liu Cui Ping, Li M W, Cui Z, Haung J R, Tian Y L, Lin T and Mi W B 2007 *J. Mater. Sci.* **42** 6133
- Maaz K, Karim S, Mumtaz A, Hasanain S K, Liu J and Duan J L 2009 *J. Magn. Magn. Mater.* **321** 1838
- Mishra S, Karak N, Kundu T K, Das D, Maity N and Chkravorty D 2006 *Mater. Letts* **60** 1111
- Montemayor S M, Garcia-Cerda L A, Torres-Lubian J R and Fernandez O S R 2007 *J. Sol-Gel Sci. Technol.* **42** 181
- Murdock E S, Simmons R F and Davidson R 1992 *IEEE Trans. Magn.* **28** 3078
- Patil D R and Chougule B K 2009 *Mater. Chem. Phys.* **117** 35
- Priyadharsini P, Pradeep A, Rao P S and Chandrasekaran G 2009 *Mater. Chem. Phys.* **116** 207
- Raming T P, Winnubst A J A, Van Kats C M and Philipse P 2002 *J. Colloid Interf. Sci.* **249** 346
- Rana S, Gallo A, Srivastava R S and Misra R D K 2007 *Acta Biomater.* **3** 233
- Satyanarayana L, Madhusudan Reddy K and Manorama S V 2003 *Mater. Chem. Phys.* **82** 21
- Singhal S and Chandra K 2007 *J. Solid State Chem.* **180** 296
- Smit J and Wijn H P J 1959 *Ferrites* (The Netherlands: Philips Technical Library) p. 137
- Waldron R D 1955 *Phys. Rev.* **99** 1727
- Yang Liufang, Xie Yongang, Zhao Heyun, Wu Xinghui and Wang Yude 2005 *Solid-State Electron.* **49** 1029
- Zahi S, Doud A R and Hashim M 2007 *Mater. Chem. Phys.* **106** 452